



**INVESTIGATION OF LASER BEAM COMBINING AND CLEAN-UP  
VIA SEEDED STIMULATED BRILLOUIN SCATTERING  
IN MULTIMODE OPTICAL FIBERS**

THESIS

Bryan J. Choi, Captain, USAF

AFIT/GEO/ENP/00M-01

**DEPARTMENT OF THE AIR FORCE  
AIR UNIVERSITY**

**AIR FORCE INSTITUTE OF TECHNOLOGY**

**Wright-Patterson Air Force Base, Ohio**

APPROVED FOR PUBLIC RELEASE; DISTRIBUTION UNLIMITED.

20001113 016

REPORT DOCUMENTATION PAGE			Form Approved OMB No. 0704-0188
Public reporting burden for this collection of information is estimated to average 1 hour per response, including the time for reviewing instructions, searching existing data sources, gathering and maintaining the data needed, and completing and reviewing the collection of information. Send comments regarding this burden estimate or any other aspect of this collection of information, including suggestions for reducing this burden, to Washington Headquarters Services, Directorate for Information Operations and Reports, 1215 Jefferson Davis Highway, Suite 1204, Arlington, VA 22202-4302, and to the Office of Management and Budget, Paperwork Reduction Project (0704-0188), Washington, DC 20503.			
1. AGENCY USE ONLY (Leave blank)	2. REPORT DATE March 2000	3. REPORT TYPE AND DATES COVERED Master's Thesis	
4. TITLE AND SUBTITLE INVESTIGATION OF LASER BEAM COMBINING AND CLEAN-UP VIA SEEDED STIMULATED BRILLOUIN SCATTERING IN MULTIMODE OPTICAL FIBERS		5. FUNDING NUMBERS	
6. AUTHOR(S) Bryan J. Choi, Capt, USAF			
7. PERFORMING ORGANIZATION NAME(S) AND ADDRESS(ES) Air Force Institute of Technology Graduate School of Engineering and Management 2950 P Street, Building 640 WPAFB, OH 45433-7765		8. PERFORMING ORGANIZATION REPORT NUMBER  AFIT/GEO/ENP/00M-01	
9. SPONSORING/MONITORING AGENCY NAME(S) AND ADDRESS(ES) Dr. Howard Schlossberg AFRL/AFOSR 801 North Randolph Street Arlington VA 22203-1977		10. SPONSORING/MONITORING AGENCY REPORT NUMBER	
11. SUPPLEMENTARY NOTES Advisor: Dr. Won B. Roh, Civ, AFIT/ENP, DSN 785-3636 ext 4509			
12a. DISTRIBUTION AVAILABILITY STATEMENT  Approved for public release; distribution unlimited		12b. DISTRIBUTION CODE	
13. ABSTRACT (Maximum 200 words) The purpose of this thesis research was to determine if stimulated Brillouin scattering amplification in multimode optical fibers would exhibit the same laser beam combining and clean-up properties exhibited by SBS oscillation, and to characterize the Brillouin amplification process in a multimode optical fiber. Beam combining in multimode fibers via SBS is being considered as a method of combining low power laser beams into a single beam having higher power and superior spatial coherence for applications such as electro-optic countermeasures. Experimental results demonstrate seeding a 9.5 mm fiber significantly reduced the pump power required to initiate SBS. An amplified Stokes beam was observed with as little as 4 mW of pump power, and the maximum conversion efficiency was 44%, similar to conversion efficiencies reported for SBS oscillation. Polarization of the Stokes beam depended on seed beam polarization. The profile of the amplified Stokes beam depended on the coupling and polarization of the seed fiber; both LP01 and LP11 modes were observed from the 9.5 mm fiber. However, the Stokes beam profile did not depend on spatial quality of the pump beam, exhibiting some of the clean-up properties associated with the SBS oscillation process.			
14. SUBJECT TERMS Stimulated Brillouin Scattering, SBS, Optical Fiber, Laser Beam Combining, Laser Beam Cleanup		15. NUMBER OF PAGES 51	16. PRICE CODE
17. SECURITY CLASSIFICATION OF REPORT Unclassified	18. SECURITY CLASSIFICATION OF THIS PAGE Unclassified	19. SECURITY CLASSIFICATION OF ABSTRACT Unclassified	20. LIMITATION OF ABSTRACT UL

The views expressed in this thesis are those of the author and do not reflect the official policy or position of the United States Air Force, Department of Defense or the U. S. Government.

AFIT/GEO/ENP/00M-01

INVESTIGATION OF LASER BEAM COMBINING AND CLEAN-UP  
VIA SEEDED STIMULATED BRILLOUIN SCATTERING  
IN MULTIMODE OPTICAL FIBERS

THESIS

Presented to the Faculty

Department of Engineering Physics

Graduate School of Engineering and Management

Air Force Institute of Technology

Air University

Air Education and Training Command

In Partial Fulfillment of the Requirements for the  
Degree of Master of Science in Electrical Engineering

Bryan J. Choi, B.S.

Captain, USAF

March 2000


Approved for public release; distribution unlimited

AFIT/GEO/ENP/00M-01


INVESTIGATION OF LASER BEAM COMBINING AND CLEAN-UP  
VIA SEEDED STIMULATED BRILLOUIN SCATTERING  
IN MULTIMODE OPTICAL FIBERS

Bryan J. Choi, B.S.  
Captain, USAF


Approved:

  
\_\_\_\_\_  
Won B. Roh (Chairman)

2 Mar 00  
date

  
\_\_\_\_\_  
Eric P. Magee (Member)

2 MAR 2000  
date

  
\_\_\_\_\_  
Craig C. Largent (Member)

2 March 00  
date

## *Acknowledgments*

There are several people without whom this thesis would not have been possible. I would like to thank my advisor, Dr. Won Roh, not only for his technical guidance, but also his patience and understanding. I would also like to thank Majors Eric Magee and Craig Largent for serving on my committee. Captain Tim Russell shared his knowledge of theory and laboratory procedures, for which I am greatly indebted. Finally, I would like to thank my family and friends for their support throughout the writing of this thesis.

## *Table of Contents*

	Page
Acknowledgments.....	iv
List of Figures .....	vii
List of Tables.....	ix
Abstract .....	x
I. Introduction.....	1
II. Background .....	4
2.1 Properties of Optical Fibers.....	4
2.2 Theory of Stimulated Brillouin Scattering .....	7
III. Previous Experimental Results.....	14
3.1 SBS in Optical Fiber .....	14
3.2 Reduction of Brillouin Threshold .....	15
3.3 Laser Beam Combining.....	16
IV. Experimental Setup .....	18
4.1 Seed Beam Generation .....	20
4.2 SBS Amplification .....	21
V. Results and Analysis .....	24
5.1 Minimum Pump Power and Conversion Efficiency .....	24
5.2 Amplifier Gain .....	26
5.3 Brillouin Shift.....	28
5.4 Beam Profile.....	28

5.5 Polarization of the Stokes Beam .....	29
5.5 SBS Amplification in 50 $\mu\text{m}$ Fiber .....	32
VI. Conclusion and Recommendations .....	34
6.1 Conclusion.....	34
6.2 Recommendations for Future Research .....	35
Bibliography.....	38
Vita.....	40

## *List of Figures*

Figure 1. Light guiding property of optical fibers (1:24).....	4
Figure 2. Mode-width parameter, $w$ , as a function of normalized frequency, $V$ (1:38). .....	6
Figure 3. Brillouin gain spectra of three different fibers: (a) silica-core, (b) depressed-cladding, and (c) dispersion-shifted fibers (1:359).....	9
Figure 4. Stokes beam growth and pump beam depletion as a function of position in the fiber. Solid lines are for $b_{in}=0.001$ and dashes lines are for $b_{in}=0.01$ (2). .....	12
Figure 5. Experimental setup used by Ippen and Stolen to observe SBS (10:539).....	14
Figure 6. SBS power measurement reported by Rodgers in Corning SMF-28(TM) fiber at 808 nm (13:60).....	16
Figure 7. Spectrum of SDL-8630 Tunable Laser Diode used in these experiments. X-axis is relative frequency and Y-axis is relative intensity in arbitrary units. ....	18
Figure 8. Experimental setup used for SBS amplification. ....	23
Figure 9. Seeded and unseeded output power as a function of pump power. ....	24
Figure 10. Amplified Stokes beam power as a function of pump power.....	25
Figure 11. Stokes output versus seed power. Pump power was 32.9 mW .....	27
Figure 12. Saturated amplifier gain as a function of seed power. Pump power was 32.9 mW.....	27
Figure 13. Spectrum of pump and Stokes beams. X-axis is relative frequency and Y-axis is relative intensity.....	28
Figure 14. Images of the output beam: (a) $LP_{01}$ seed beam without pumping, (b) amplified $LP_{01}$ beam, (c) $LP_{11}$ seed beam without pumping, and (d) amplified $LP_{11}$ beam.....	30
Figure 15. Profile of the Fresnel reflection of the pump beam: (a) unaberrated beam and (b) aberrated beam. ....	31

Figure 16. Effects of seed beam polarization on the amplified Stokes beam: (a) amplifier output for an arbitrary rotation of the seed beam polarization and (b) amplifier output when seed beam polarization has been rotated by 90 degrees. .... 32

Figure 17. Contour plots of amplifier output for the 50  $\mu\text{m}$  fiber: (a) Fresnel reflection, (b) seed beam only, and (c) amplifier output with maximum pump power applied. SBS does not occur in the 50  $\mu\text{m}$  fiber. .... 33

*List of Tables*

Table 1. Parameters for 9.5  $\mu\text{m}$  and 50  $\mu\text{m}$  fibers used. .... 20

*Abstract*

The purpose of this thesis research was to determine if stimulated Brillouin scattering (SBS) amplification in multimode optical fibers would exhibit the same laser beam combining and clean-up properties exhibited by SBS oscillation, and to characterize the Brillouin amplification process in a multimode optical fiber. Beam combining in multimode fibers via SBS is being considered as a method of combining low power laser beams into a single beam having higher power and superior spatial coherence for applications such as electro-optic countermeasures.

Experimental results demonstrate seeding a 9.5  $\mu\text{m}$  fiber significantly reduced the pump power required to initiate SBS. An amplified Stokes beam was observed with as little as 4 mW of pump power, and the maximum conversion efficiency was 44%, similar to conversion efficiencies reported for SBS oscillation. Polarization of the Stokes beam depended on seed beam polarization.

The profile of the amplified Stokes beam depended on the coupling and polarization of the seed fiber; both  $\text{LP}_{01}$  and  $\text{LP}_{11}$  modes were observed from the 9.5  $\mu\text{m}$  fiber. However, the Stokes beam profile did not depend on spatial quality of the pump beam, exhibiting some of the clean-up properties associated with the SBS oscillation process.

INVESTIGATION OF LASER BEAM COMBINING AND CLEAN-UP  
VIA SEEDED STIMULATED BRILLOUIN SCATTERING  
IN MULTIMODE OPTICAL FIBERS

*I. Introduction*

The Air Force has identified and is pursuing the role of lasers in electro-optic countermeasures, remote sensing, and target illumination and tracking. Increasing optical power enhances the capabilities of such systems in terms of extended range and effectiveness. Current high and moderate power laser systems can be large and inefficient, requiring substantial maintenance. Such systems may be suitable for ground-based systems, but are certainly not desirable or even feasible for airborne or space-based systems. In contrast, semiconductor lasers are small, efficient, and reliable, but are incapable of individually producing more than, at most, a few watts of optical power. Efficiently combining many semiconductor lasers would create a system with the advantages of an individual semiconductor laser, but with the ability to produce several hundreds of watts of optical power. The small size and weight of hundreds of semiconductor lasers is much less than that of a comparable solid-state, gas, or liquid laser. Other benefits of a combined diode laser system over conventional lasers include reduced cost and increased redundancy.

A method of combining multiple laser beams utilizes stimulated Brillouin scattering (SBS) oscillation in optical fibers to coherently combine laser beams. The

results from previous research indicate that the output beam generated via SBS efficiently converted the power of two incident lasers into a spatially coherent fundamental gaussian-like beam (14). A spatially coherent gaussian beam is essential for directed energy applications to maximize energy in as small an area as possible. Extending this research will provide additional insight into the possibility of producing kilowatt power laser systems by combining many lower power diode lasers.

Using SBS in an optical fiber to combine beams takes advantage of high intensity of light within the core of the fiber, long interaction length, and the light guiding nature of optical fibers. One way of further increasing the efficiency of this beam combining method is to utilize SBS as an amplification process rather than an oscillation process. This can be accomplished by seeding the back end of the fiber with light of the appropriate Stokes frequency. Because of the Brillouin shift associated with the SBS process, the seed beam must precisely match the frequency of the Stokes beam generated via SBS. To generate this seed beam for this thesis, a portion of the pump laser was used to excite SBS oscillation in a second spool of identical optical fiber. This ensured the seed beam would precisely match the Stokes frequency within the amplifier fiber.

It was expected that seeding the amplifier will reduce the amount of pump power required to observe a measurable SBS beam, based on information for fiber Brillouin amplifiers given by Agrawal (2:281-283). However, the beam cleaning property of the SBS amplification process had not been investigated thus far.

This thesis begins in Chapter II with background information regarding optical fibers and the theory behind SBS. In Chapter III, previous work in SBS, SBS beam combining, and SBS amplification are summarized. Chapter IV describes the equipment

used and experimental setup. Results and analysis of the data are presented in Chapter V. The thesis concludes with Chapter VI, which also presents some recommendations for future research in this area.

## II. Background

This chapter will describe the theory of SBS in optical fibers. Rudimentary knowledge of the properties of step-index optical fibers and of general SBS theory is critical to understanding the experiments performed for this thesis.

### 2.1 Properties of Optical Fibers

The optical fibers used in these experiments were all of the step-index type, and, for simplicity, only properties of step-index fibers will be discussed. Step-index optical fibers consist of a central core of index  $n_1$  surrounded by a cladding of index  $n_2$ . An outer layer, called the jacket, is typically added to protect the fiber. Such fibers rely on total internal reflection at the core-cladding interface to guide light down the core of the fiber as shown in Figure 1.

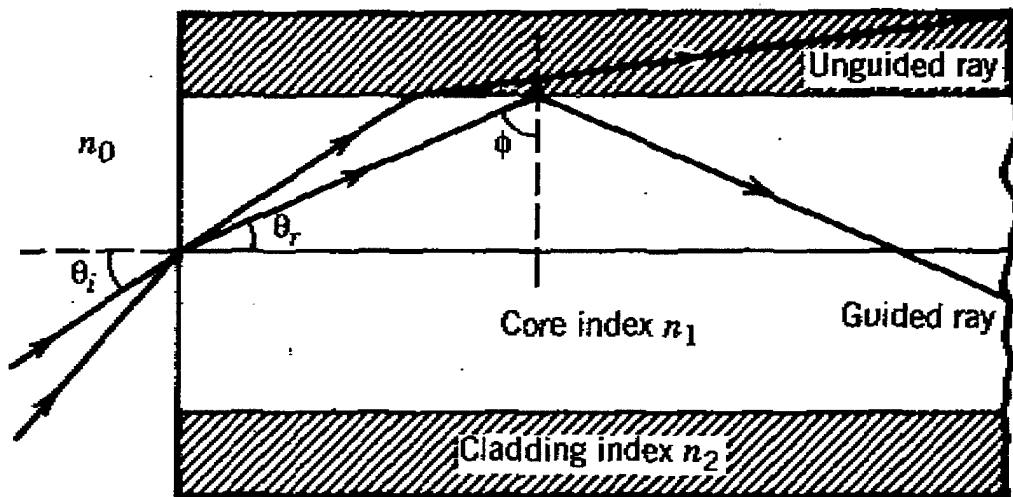


Figure 1. Light guiding property of optical fibers (1:24).

The numerical aperture (NA) of a fiber is determined by the critical angle at the core-cladding interface, which, in turn, defines the angle of acceptance for light to be coupled into the fiber,  $\theta_{1/2}$  (denoted as  $\theta_i$  in Figure 1),

$$NA = \sqrt{n_1^2 - n_2^2} \quad (1)$$

$$\theta_{1/2} \leq \sin^{-1}(NA) \quad (2)$$

To couple light into an optical fiber, light is focused onto the end of the fiber. There is a minimum constraint on the focal length of the coupling optics in order to ensure all incident light is within the numerical aperture of the fiber. However, the diffraction limited spot size of the focused beam is directly proportional to this focal length

$$d_{SPOT} = \frac{2.44\lambda f}{D} \quad (3)$$

where  $\lambda$  is the wavelength,  $f$  is the focal length of the coupling optics, and  $D$  is the diameter of the incident beam. Clearly, in order to maximize coupling efficiency,  $d_{SPOT}$  should be no larger than the core diameter of the optical fiber. Thus, the focal length of the coupling optics must be carefully selected to satisfy constraints of both numerical aperture and core diameter of the fiber.

The normalized frequency,  $V$ , of a fiber determines the number of modes supported by the fiber. It is given by

$$V = \frac{\pi d_{FIBER}}{\lambda} NA \quad (4)$$

where  $d_{FIBER}$  is the core diameter of the fiber. For  $V < 2.405$ , the fiber will only support one mode. The actual number of modes supported by the fiber for large  $V$  is given by

$$N \approx \frac{V^2}{2} \quad (5)$$

The normalized frequency is also used to determine the effective core area.

Assuming the fundamental fiber mode is gaussian, Figure 2 shows the dependence of the mode-width parameter,  $w$ , on  $V$ . The effective core area can be calculated based on  $w$  as

$$A_{eff} = \pi w^2 \quad (6)$$

Losses in the fiber due predominantly to absorption by the medium and Rayleigh scattering reduce the amount of power transmitted through long lengths of fiber. This is accounted for by using the effective length of a fiber in transmission calculations. For a fiber of physical length  $L$ , the effective length,  $L_{eff}$ , is given by

$$L_{eff} = \frac{1 - e^{-\alpha L}}{\alpha} \quad (7)$$

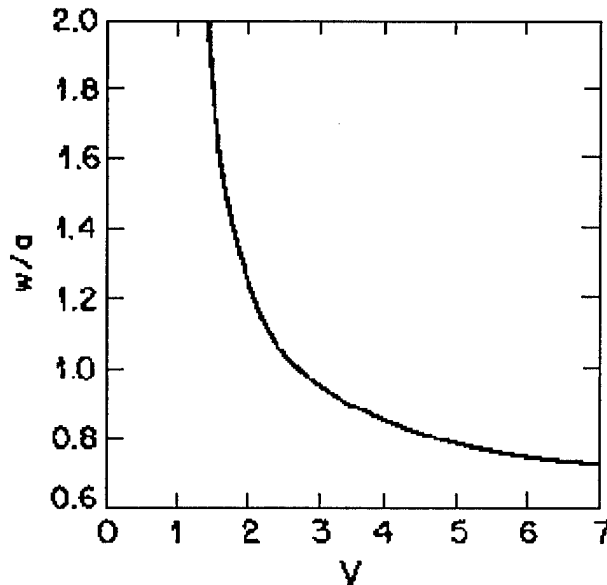


Figure 2. Mode-width parameter,  $w$ , as a function of normalized frequency,  $V$  (1:38).

The loss coefficient,  $\alpha$ , is typically given by the manufacturer, but can also be calculated using

$$P(L) = P(0)C_0e^{-\alpha L} \quad (8)$$

where  $P(0)$  is the power incident on the coupling optics,  $P(L)$  is the power transmitted through the fiber, and  $C_0$  is the coupling efficiency. The loss coefficient can be given in units of dB/m or  $m^{-1}$ ; in these equations the latter is used, and the conversion between the two is given by (16:297)

$$\alpha = .23\alpha_{dB} \quad (9)$$

The coupling efficiency,  $C_0$ , defines the amount of light that successfully enters the core and is guided through the fiber. This is calculated empirically by measuring the amount of light incident on the coupling lens and the amount of light which is transmitted through approximately two meters of optical fiber. Two meters is selected since fiber loss can be neglected and most of the light which is not coupled into a guiding mode of the fiber has already exited through the cladding.

## 2.2 Theory of Stimulated Brillouin Scattering

Classically, stimulated Brillouin scattering (SBS) is a non-linear optical phenomenon in which a portion of laser power incident on an optical medium is converted to a second beam, slightly shifted in frequency. This second beam is known as the Stokes beam. The incident pump laser beam generates an acoustic wave in the medium through the process of electrostriction, which causes an index grating to form in the medium due to the longitudinal nature of the acoustic wave (8). This induced grating scatters the pump beam by Bragg reflection via elasto-optic phenomenon, generating the Stokes beam. The

interaction of these three waves must satisfy the laws of conservation of energy and momentum, and are related by

$$\omega_A = \omega_P - \omega_S \quad (10)$$

$$\mathbf{k}_A = \mathbf{k}_P - \mathbf{k}_S \quad (11)$$

where  $\omega$  is the angular frequency and  $\mathbf{k}$  is the momentum of the respective beams. In bulk media, there is no constraint on the direction of propagation of the Stokes beam. However, in optical fibers, the guiding nature of the fiber restricts propagation to the forward or backward direction. Since the acoustic wave must satisfy the dispersion relation (2:264)

$$\omega_A = 2v_A |\mathbf{k}_P| \sin\left(\frac{\theta}{2}\right) \quad (12)$$

SBS does not occur in the forward direction and only the backward propagating Stokes beam is considered. Thus, the Stokes beam is slightly lower in frequency than the pump beam in accordance with Equation 10. The frequency of the Brillouin shift is given by

$$\nu_B = \frac{2n v_A}{\lambda_p} \quad (13)$$

where  $n$  is the index of refraction ( $\sim 1.45$  for silica fiber),  $v_A$  is the speed of the acoustic wave ( $\sim 5.96$  km/s for silica fiber), and  $\lambda_p$  is the wavelength of the pump beam.

The growth of the Stokes wave depends on the Brillouin-gain coefficient,  $g_B(\nu)$ . The peak value of the Brillouin-gain coefficient occurs for  $\nu = \nu_B$ , and the spectral width, denoted by  $\Delta\nu_B$ , is related to the acoustic phonon lifetime,  $\Delta\nu_B = (\pi T_B)^{-1}$ . If the acoustic wave generated through electrostriction decays exponentially, the Brillouin-gain coefficient takes a Lorentzian profile given by (1:358)

$$g_B(\nu) = \frac{(\Delta\nu_B/2)^2}{(\nu - \nu_B)^2 + (\Delta\nu_B/2)^2} g_B(\nu_B) \quad (14)$$

The peak value of the Brillouin-gain coefficient at  $\nu_B$  is given by (1:359)

$$g_B(\nu_B) = \frac{2\pi n^7 p_{12}^2}{c \lambda_p^2 \rho_0 v_A \Delta\nu_B} \quad (15)$$

where  $p_{12}$  is the longitudinal elasto-optic coefficient and  $\rho_0$  is the density of the medium.

While Equation 15 shows the Brillouin-gain coefficient inversely proportional to  $\lambda^2$ , this dependence is offset by the fact that  $\Delta\nu_B$  is also inversely proportional to  $\lambda^2$ ; thus, the peak Brillouin-gain coefficient is nearly independent of the pump wavelength. The commonly accepted value of the Brillouin-gain coefficient in fused silica is  $5E-11$  m/W (2:266).

The spectral width of the Brillouin-gain coefficient is typically on the order of tens of megahertz. In optical fibers, the spectral width depends on the presence of dopants in the fiber core and differs from the spectral width in bulk silica due to the

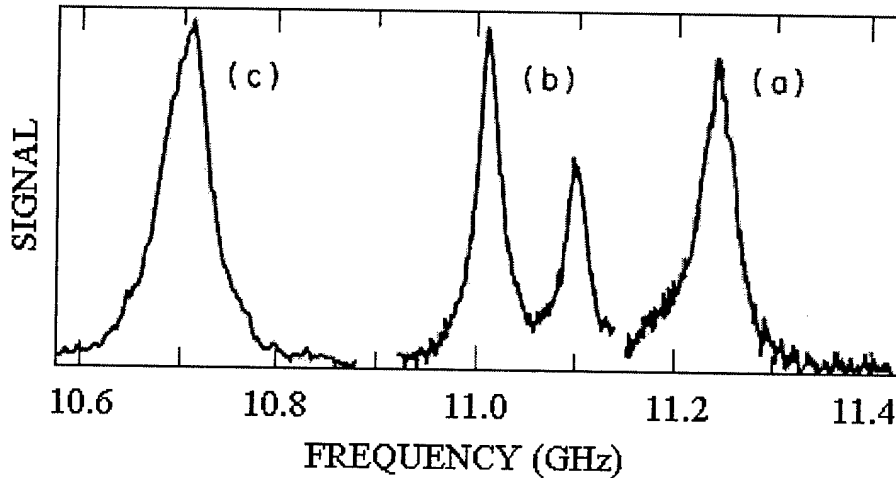


Figure 3. Brillouin gain spectra of three different fibers: (a) silica-core, (b) depressed-cladding, and (c) dispersion-shifted fibers (1:359).

guiding nature of the fibers. Figure 3 shows the Brillouin-gain coefficient as a function of frequency for three different fibers at a pump wavelength of 1.525  $\mu\text{m}$ .

As mentioned previously, the Stokes wave is generated through the interaction between the pump beam and the acoustically induced index grating. Equation 14 assumes a cw or quasi-cw pump beam. For a pulsed pump beam, if the pulse width,  $T_0$ , is less than the phonon lifetime,  $T_B$ , then the Brillouin gain is significantly reduced. For pump pulse width less than 1 ns, SBS is suppressed, and stimulated Raman scattering becomes the dominant non-linear phenomenon. The acoustic phonons cannot respond quickly enough to the short pulses, so their interaction which results in SBS is significantly reduced. In the case where the spectral width of the pump exceeds that of the Brillouin gain, the peak gain coefficient is reduced and is given by (1:360)

$$\tilde{g}_B = \frac{\Delta\nu_B}{\Delta\nu_B + \Delta\nu_P} g_B(\nu_B) \quad (16)$$

where  $\Delta\nu_B$  and  $\Delta\nu_P$  are the Brillouin gain spectral width and pump spectral width, respectively.

The relationship between the Stokes beam and the pump beam intensities in steady state is governed by (2:268)

$$\frac{dI_S}{dz} = -g_B I_P I_S + \alpha I_S \quad (17)$$

$$\frac{dI_P}{dz} = -g_B I_P I_S - \alpha I_P \quad (18)$$

where  $g_B$  is the Brillouin-gain coefficient and  $\alpha$  is the loss coefficient of the fiber. While the loss coefficient depends on wavelength, it is convenient to assume it is the same for both pump and Stokes wavelengths since  $\lambda_P \cong \lambda_S$ .

To determine the pump power above which SBS will occur, pump depletion in the fiber can be neglected, and Equations 17 and 18 can be solved to relate the Stokes power exiting the front of the fiber to the Stokes beam incident at the end of the fiber (2:268)

$$I_S(0) = I_S(L) e^{\frac{g_B P_0 L_{eff}}{A_{eff}} - \alpha L} \quad (19)$$

For SBS oscillation,  $I_S(L)$  is generated by a fictitious Stokes photon due to noise or spontaneous Brillouin scattering. For SBS oscillation, the minimum pump power is known as the Brillouin threshold, which can be approximated by (2:269)

$$\frac{g_B P_0^{cr} L_{eff}}{A_{eff}} \approx 21 \quad (20)$$

where  $P_0^{cr}$  is the Brillouin threshold power. The factor of 21 is approximate and depends on both the value of the Brillouin-gain line width and the amount of depolarization that occurs in the fiber. For complete depolarization, this factor doubles.

When determining the growth of the Stokes beam once the pump is above the Brillouin threshold, pump depletion must be taken into account, and the solutions to Equations 17 and 18 are given by (2:270)

$$I_S(z) = \frac{b_0(1-b_0)}{G(z)-b_0} I_P(0) e^{-\alpha z} \quad (21)$$

$$I_P(z) = \frac{(1-b_0)G(z)}{G(z)-b_0} I_P(0) e^{-\alpha z} \quad (22)$$

where

$$G(z) = e^{(1-b_0)\left(\frac{g_0}{\alpha}\right)(1-e^{-\alpha z})} \quad (23)$$

$$b_0 = \frac{I_S(0)}{I_P(0)} \quad (24)$$

$$g_0 = g_B I_P(0) \quad (25)$$

The Stokes and pump intensities as a function of  $z$  for certain parameters is shown in Figure 4. The relative input intensity is denoted by the parameter  $b_{in}$ , which is defined as

$$b_{in} = \frac{I_S(L)}{I_P(0)} \quad (26)$$

The solid lines represent the case where  $b_{in}=0.001$ , while the dashed lines represent the

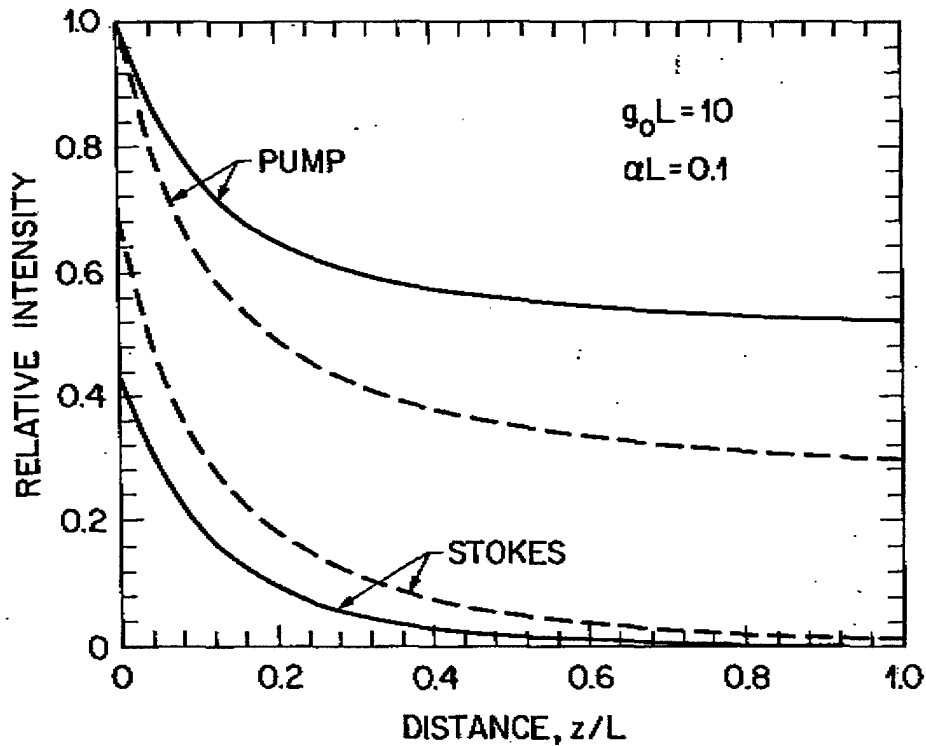


Figure 4. Stokes beam growth and pump beam depletion as a function of position in the fiber. Solid lines are for  $b_{in}=0.001$  and dashes lines are for  $b_{in}=0.01$  (2:270).

case where  $b_{in}=0.01$ . In both cases, the Brillouin gain,  $g_0L$ , was 10, and fiber loss,  $\alpha L$ , was 0.1. Most of the power transferred between the pump and Stokes beam occurs in the first 20% of the fiber length.

SBS amplification can be analyzed using Equations 21 and 22. Instead of relying on noise or spontaneous Brillouin scattering to initiate the SBS process, a seed beam is coupled into the back end of the fiber. The unsaturated gain of the system is given by (2:271)

$$G_A = e^{g_0L_{eff}} \quad (27)$$

When the Stokes beam power increases, the gain becomes saturated, and the saturated gain is given by

$$G_s = \frac{I_s(0)}{I_s(L)e^{-\alpha L}} \quad (28)$$

### III. Previous Experimental Results

Stimulated Brillouin scattering in optical fibers was initially seen as a detrimental non-linear phenomenon that would limit the amount of power transmitted through an optical fiber. While SBS does pose potential problems for fiber optic communications, some research of SBS in optical fibers can also be used to utilize the beneficial aspects of SBS. This chapter will highlight some of this research.

#### 3.1 SBS in Optical Fiber

Stimulated Brillouin scattering in optical fibers was first observed in 1972 by Ippen and Stolen (10). Their experimental setup is shown in Figure 5. Using a pulsed xenon laser at 535.5 nm as the pump laser and a 3.8  $\mu\text{m}$  diameter single-mode fiber, they reported the Brillouin gain as  $4.6\text{E-}9$  cm/W with a frequency shift of 32.2 GHz. They also estimated the SBS linewidth to be 103 MHz, significantly higher than that found for bulk

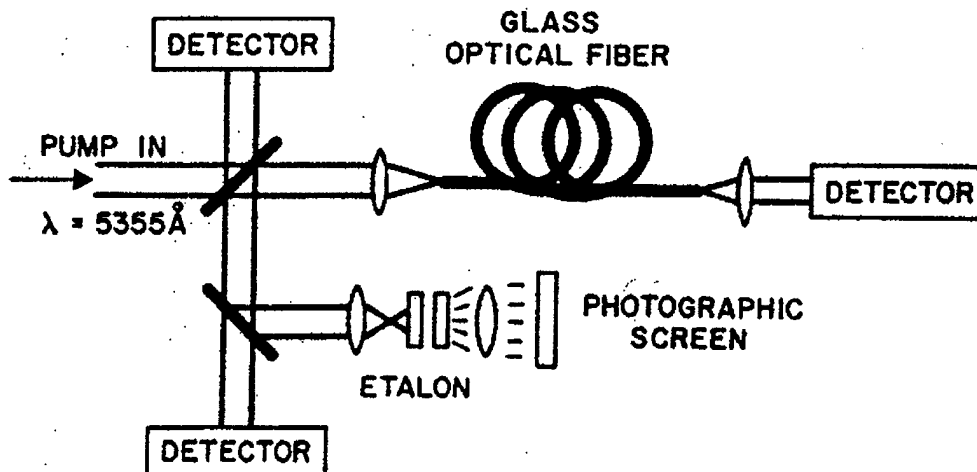


Figure 5. Experimental setup used by Ippen and Stolen to observe SBS (10:539).

silica. The threshold power for SBS in the 5.8 meter long fiber was given as 2.3 watts. Stolen later showed the dependence of the Brillouin threshold condition, given by Equation 20, on polarization of the beam within the optical fiber (18). For complete depolarization, he determined the factor of 21 on the right side of Equation 20 is multiplied by a factor of 2.

### *3.2 Reduction of Brillouin Threshold*

Reduction of the threshold power through feedback has been investigated by Hill (9), Rodgers (13), (14), and Wong (21). Hill et al. utilized a ring cavity configuration to implement a Brillouin ring laser. Using a xenon laser at 535.5 nm and a 2.4  $\mu\text{m}$  diameter, 9.5 m long single-mode fiber, with approximately 2% feedback into the back end of the fiber, he was able to reduce the SBS threshold from 550 mW to 250 mW with a conversion efficiency of 50%. Rodgers performed a similar experiment and was able to reduce the SBS threshold from 26.5 mW in a single-pass configuration to 21 mW for the ring cavity configuration. Conversion efficiency also increased from 42% to 50%, respectively. Results from Rodger's experiment is shown in Figure 6.

The development of low loss optical fibers has dramatically reduced the Brillouin threshold in long fibers. Fibers used in the early 1970s typically had losses on the order of 1000 dB/km. Today, fibers optimized for optical communications at wavelengths of 1.3  $\mu\text{m}$  and 1.55  $\mu\text{m}$  can have losses less than 1 dB/km. In 1987, Aoki et al. reported the Brillouin threshold to be 9 mW in a 30 km optical fiber with fiber loss of 0.46 dB/km at the pump wavelength of 1.3  $\mu\text{m}$  (3), (4). Cotter measured a Brillouin threshold of  $\sim$ 5 mW in a 13.6 km fiber with fiber loss of 0.41 dB/km at the wavelength of interest (6). These

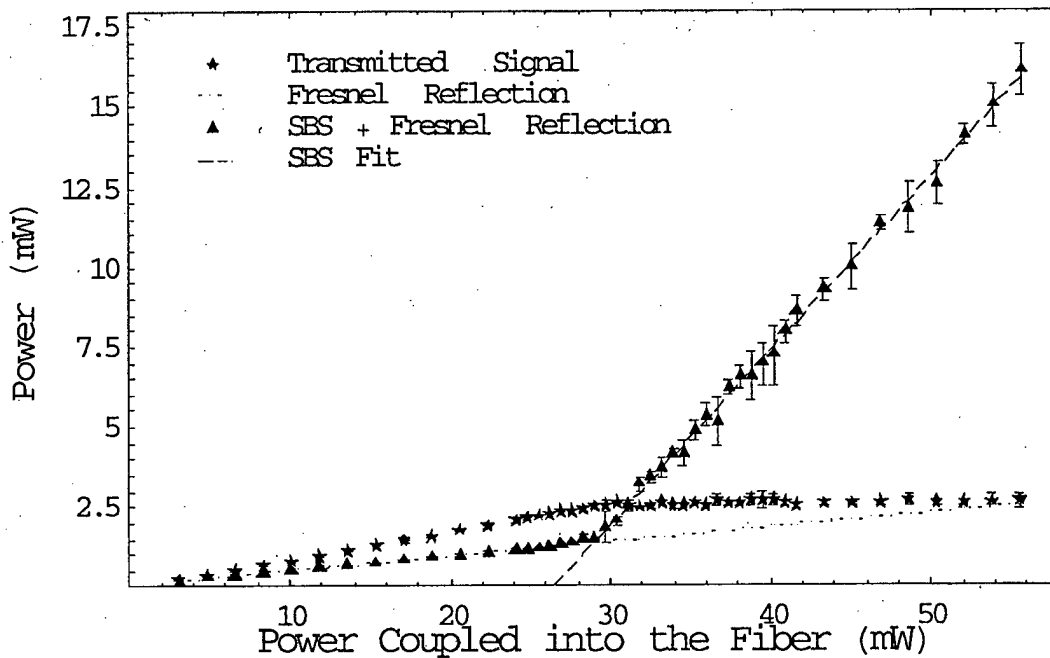


Figure 6. SBS power measurement reported by Rodgers in Corning SMF-28(TM) fiber at 808 nm (13:60).

results have shown that semiconductor lasers of only tens of milliwatts are more than capable of generating SBS in long lengths of low loss optical fiber.

### 3.3 Laser Beam Combining

SBS has also been investigated as a method for laser beam combining. Work by Valley et al. in 1986 demonstrated two beam combining and phase conjugation in a methanol SBS cell (19). Loree et al. extended this research by seeding the back end of a SF<sub>6</sub> SBS cell with a broadband pump beam which encompassed the Stokes shifted frequency (12). Rodgers et al. demonstrated beam combining via SBS in optical fibers in 1998 (14).

While Loree et al. reported a reduction in Brillouin threshold due to seeding, the experiment was performed in a bulk SBS SF<sub>6</sub> cell and did not examine the quality of the Stokes beam. Rodgers (14) and Bruesselbach (5) observed that SBS in long lengths of multimode optical fiber cleaned up an aberrated pump beam. This thesis will quantify the reduction in Brillouin threshold in a multi-mode optical fiber due to seeding and determine whether this process also exhibits beam clean up properties.

#### IV. Experimental Setup

The laser used for these experiments was a SDL-8630 external cavity Tunable Laser Diode. The laser was tunable from 803 nm to 828 nm and able to produce in excess of 500 mW of power. The laser was tuned to operate at  $815 \pm 1$  nm. Output of the laser was polarized horizontally with respect to the optical bench, with a spot size of approximately 5 mm. Wavelength of the laser was measured by a Burleigh WA-10 wavemeter, which had an accuracy of  $\pm 0.003$  nm. The spectrum of the laser and Stokes beam was observed using a Burleigh SA-10 scanning Fabry-Perot interferometer tied to a Lecroy 9450 oscilloscope. The interferometer had a free spectral range of 8 GHz and a finesse of 200.

The manufacturer claimed the laser could operate in a single longitudinal mode, with linewidth less than 50 MHz. However, during normal operation, it was difficult to

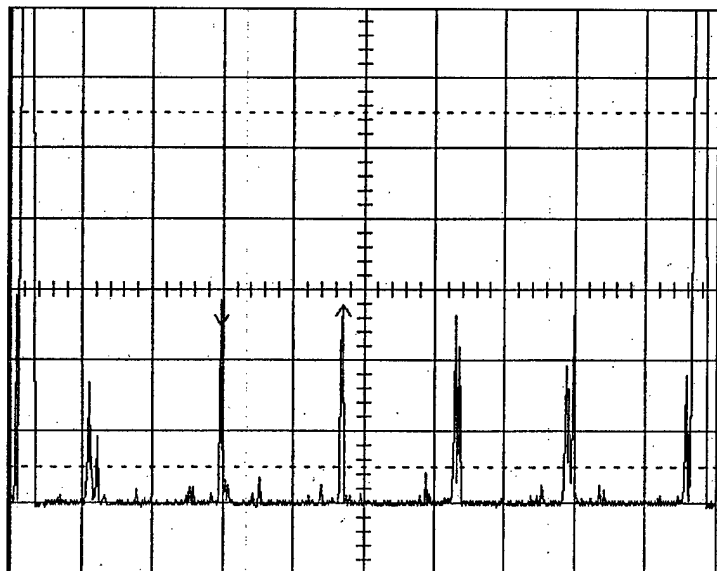


Figure 7. Spectrum of SDL-8630 Tunable Laser Diode used in these experiments. X-axis is relative frequency and Y-axis is relative intensity in arbitrary units.

force the laser into single-mode operation as shown in Figure 7. The linewidth of the primary peak varied from 50 MHz to 150 MHz, and the energy was distributed across several different lasing modes. Additionally, the frequency of the laser drifted appreciably during normal operation as measured by the interferometer and wavemeter.

Laser power was measured with a detector integrated into the laser housing using the calibration factor provided by the manufacturer. Power measurements at other locations on the bench were performed with Newport Model 815 power meters calibrated against the detector in the laser housing.

An Optics for Research IO-5-NIR optical isolator was used in order to prevent the Stokes signal from back-propagating into the laser cavity. The isolator provided approximately 35 dB attenuation at 815 nm.

Intensity profiles of the beam were captured using Coherent Beamcode 6.2 software and a Coherent CoHu 48 camera. Spatial quality and shape of the Stokes beam were determined from these contour plots.

Two different types of optical fiber were used for these experiments. The seed fiber as denoted in the experimental setup in Figure 8 was a 4.4 km spool of Corning SMF-28(TM) optical fiber with a 9.5  $\mu\text{m}$  core. The amplification fiber for the first experiment was a second spool of the same fiber. For the second experiment, a 4.4 km spool of Corning 50/125 optical fiber was used. The fiber parameters are listed in Table 1 below.

The loss coefficient for the 9.5  $\mu\text{m}$  fiber was determined using Equation 8 and experimentally measuring the coupling efficiency as 0.241 for the front end of the amplifier fiber.

Table 1. Parameters for 9.5  $\mu\text{m}$  and 50  $\mu\text{m}$  fibers used for SBS amplification.

	Corning SMF-28(TM)	Corning 50/125 Fiber
Core Diameter	9.5 $\mu\text{m}$	50 $\mu\text{m}$
Length	4.4 km	4.4 km
Loss Coefficient	2.25 dB/km	2.3 dB/km
Numerical Aperture	0.12	0.22

The ends of the fibers were held in Newport FP-1 or FP-2 fiber-optic positioners which provided at least 3 degrees of freedom. Light was coupled into the fibers using 10X microscope objectives.

#### 4.1 Seed Beam Generation

In order to initiate SBS in the amplification fiber, a seed beam at precisely the Stokes frequency was required. In order to avoid confusion, the beam generated by SBS in the seed fiber will henceforth be called the seed beam, while the beam generated by amplification will be called the Stokes beam.

A portion of the pump laser power was split off using a 50/50 beamsplitter and directed towards a spool of fiber which is denoted as the seed fiber in Figure 8. The half-wave plate used in conjunction with the polarizing beamsplitter in that leg of the optical system was used to control the amount of pump power used for seed beam generation; rather than adjust the overall pump laser power, this method allowed for independent control of pump power for both seed and amplifier fibers. The polarizing beamsplitter transmitted only the portion of the beam that was horizontally polarized.

A Faraday rotator (Optics for Research IO-10-810-1) and quarter-wave plate were used to exploit the polarization of the seed beam to isolate it from the Fresnel reflection from the end of the fiber. Rodgers demonstrated that the Stokes beam generated via SBS using a circularly polarized pump beam would not change handedness as would the Fresnel reflection (13). Thus, the Fresnel reflection passing back through the quarter-wave plate and Faraday rotator would be horizontally polarized and pass through the beamsplitter, whereas the seed beam generated through SBS would be vertically polarized and would be reflected at the beamsplitter. This method was used only to separate the Fresnel reflection from the seed beam and not in the amplifier fiber itself.

The power of the seed beam was monitored by measuring the Fresnel reflection off a microscope slide placed close to the back end of the amplifier fiber.

#### *4.2 SBS Amplification*

The remaining power that was not directed into the seed fiber was directed into the front end of the fiber used for amplification. Again, a half-wave plate and polarizing beamsplitter combination was utilized to independently adjust pump power. A 1/4" thick parallel glass plate was used to reflect a portion of the pump beam as well as a portion of the beam propagating in the backward direction. This plate was placed at approximately 45 degrees to maximize the separation between the reflections off the front and back surfaces of the plate. The reflections in the forward direction were used to measure pump power. One reflection from the backward propagating beam was picked off by a mirror and directed into the interferometer, while the second beam was sent through a polarizer and into the Beamcode camera. For gain measurements, a power meter intercepted both reflections of the backward propagating beam.

This experimental setup was used for SBS amplification in both 9.5  $\mu\text{m}$  and 50  $\mu\text{m}$  optical fibers as the amplifier fiber.

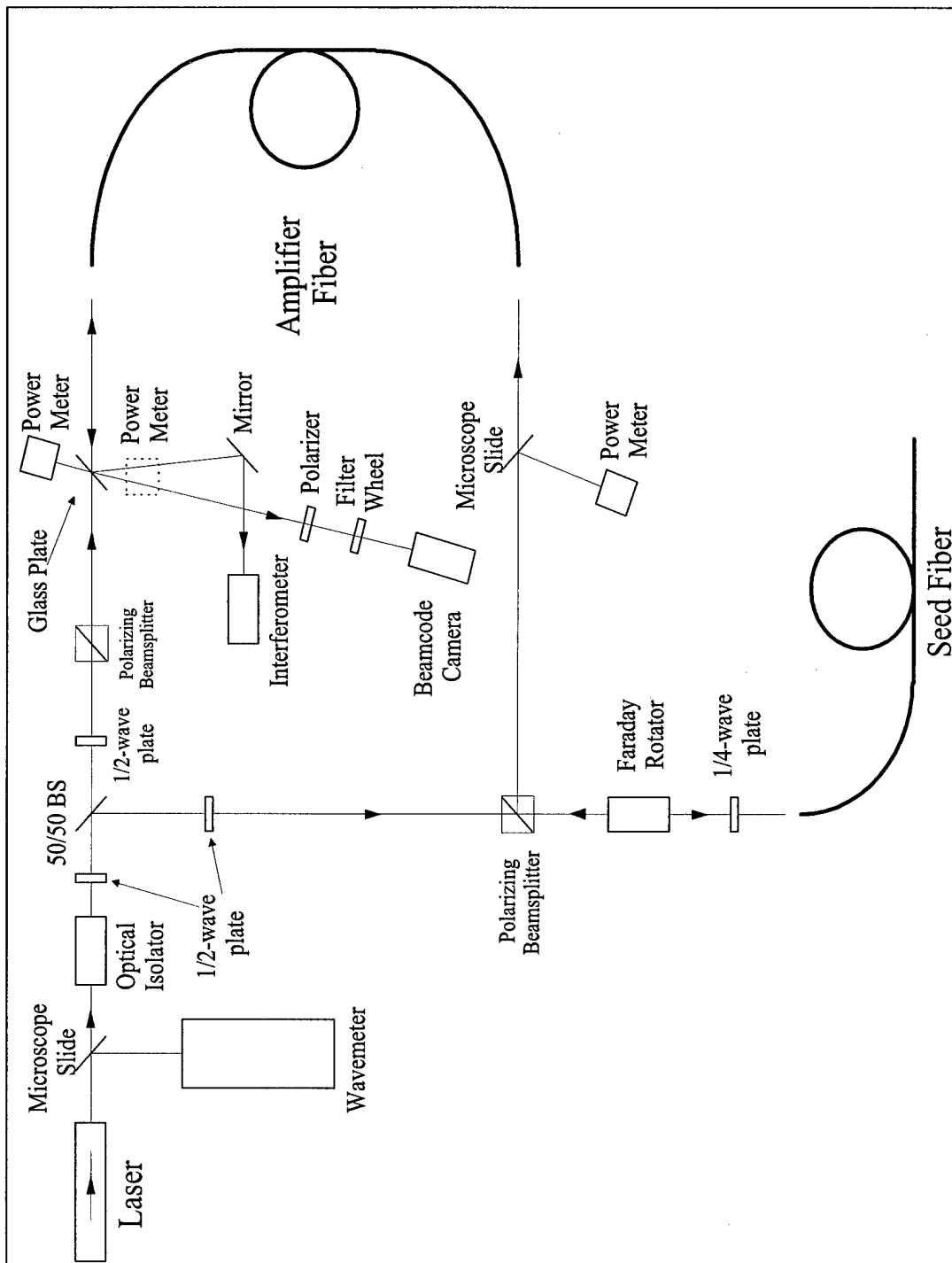


Figure 8. Experimental setup used to demonstrate SBS amplification.

## V. Results and Analysis

Results from the 9.5  $\mu\text{m}$  amplifier fiber are presented, with discussion of the pump power required for SBS amplification, conversion efficiency, beam profile, and polarization. This is followed by a brief discussion of attempts to observe SBS amplification in the 50  $\mu\text{m}$  fiber.

### 5.1 Minimum Pump Power and Conversion Efficiency

A plot of seeded and unseeded SBS amplification in the 9.5  $\mu\text{m}$  fiber is shown in Figure 9. Seed power coupled into the fiber was  $2.3 \pm 0.22$  mW. SBS did not occur when the fiber was unseeded, and only the Fresnel reflection from the fiber face is observed. In the seeded case, the output beam consisted of the sum of the Fresnel

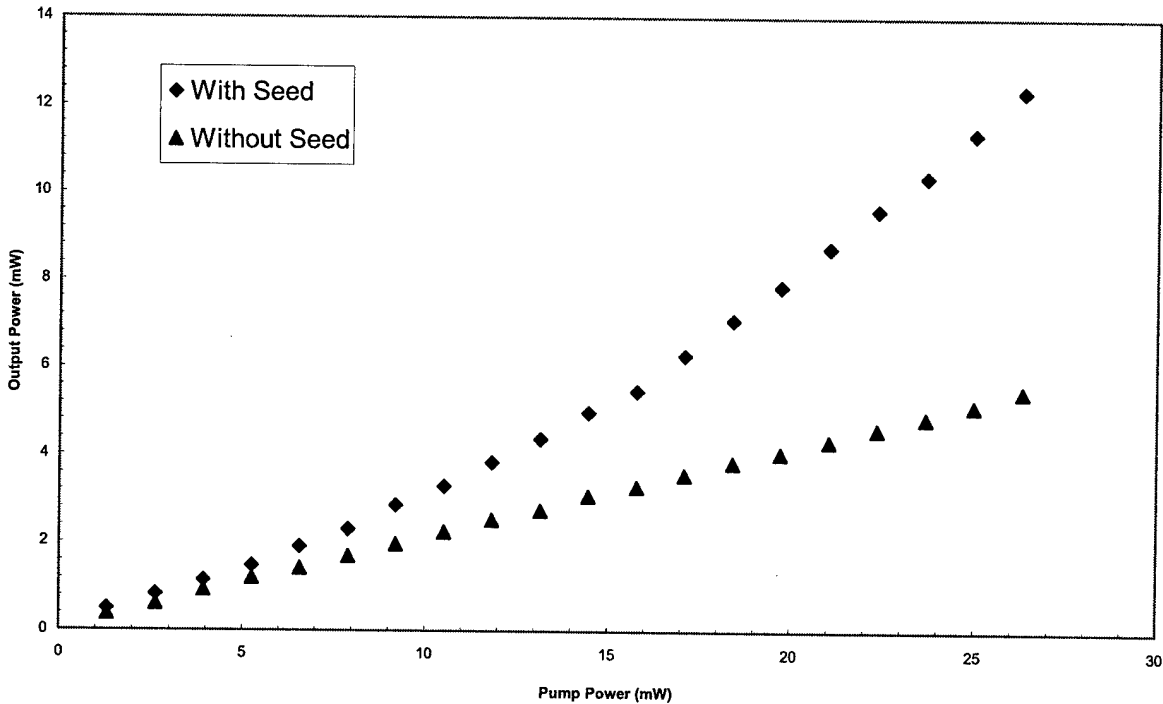


Figure 9. Seeded and unseeded output power as a function of pump power.

reflection, the portion of the seed beam which has transmitted through the amplifier fiber (after fiber losses), and the Stokes beam generated via SBS. From this graph, it is clear that SBS amplification (the case with the seed beam) occurs, while SBS oscillation (absence of the seed beam) for the same pump powers does not occur.

The Stokes beam power can be calculated by subtracting the portion due to Fresnel reflection and the amount of seed power transmitted through the optical fiber. This is shown in Figure 10. Two least-squares linear curves have been added to determine the conversion efficiency and minimum pump power for which SBS occurs. The solid line indicates a conversion efficiency of  $44.0 \pm 0.1\%$ , nearly identical to efficiencies reported for single-pass SBS oscillation. Although this line indicates the

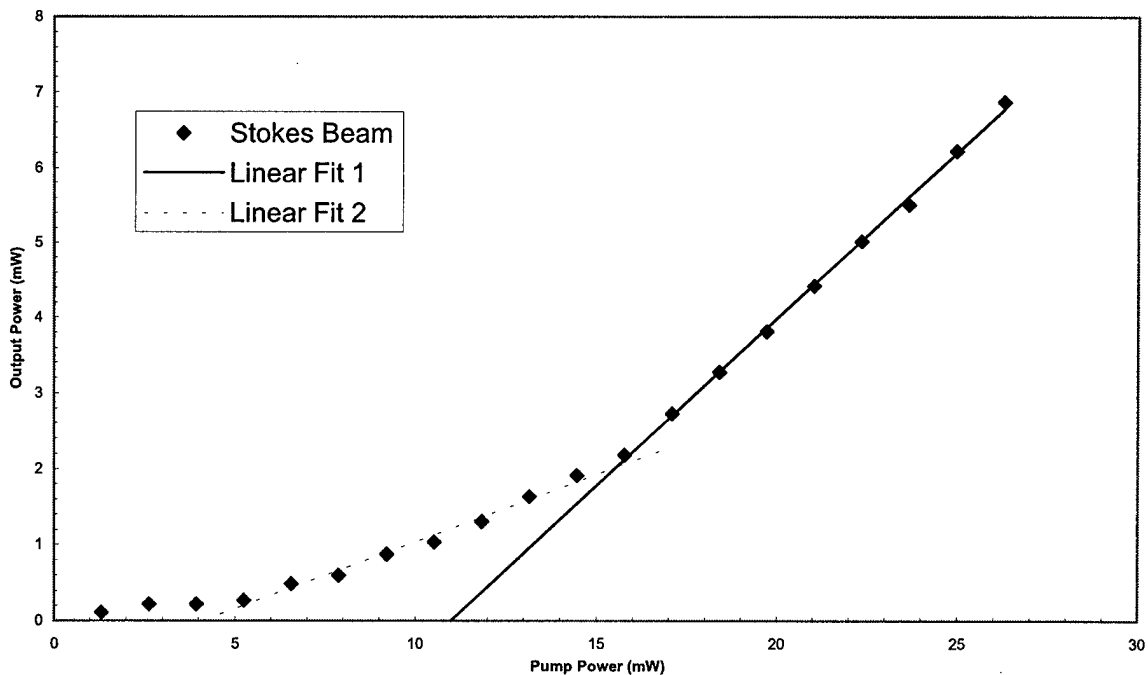


Figure 10. Amplified Stokes beam power as a function of pump power.

minimum pump power for SBS of approximately 11 mW, there is an initial increase in output power which occurs when the pump exceeds approximately 4 mW. The dashed line fits this data and has been extrapolated to show a threshold of 4.10 mW. The Brillouin threshold is defined by Agrawal as the power at which pump and Stokes power at the fiber output are approximately equal (2:222). By modifying Equation 19 accordingly and solving it numerically, the minimum pump power to support SBS amplification is estimated to be 4.33 mW.

Seeding the fiber aids in the onset of SBS by decreasing the amount of pump power required, but does not improve conversion efficiency when pump power is much larger than seed power. When the pump power is small relative to the seed power, the seed beam enhances the Stokes output as shown by the dashed line in Figure 10. However, as pump power increases and becomes much larger than the seed power, the presence of the seed beam in terms of Stokes power is dominated by the conversion of pump photons, and the conversion efficiency at high pump powers approaches that for SBS oscillation as shown by the solid line.

## *5.2 Amplifier Gain*

The small signal gain of the SBS amplifier with 32.9 mW of pump power is calculated from Equation 27 to be  $9.3E24$ , or approximately 250 dB. For the seed powers used in these experiments, however, Equation 28 applies since the gain is saturated. Figure 11 shows a plot of output power versus seed power for pump power of 32.9 mW. The non-uniform data points were unavoidable since the seed beam generated by SBS oscillation exhibited fluctuations in intensity and could not be accurately adjusted to a

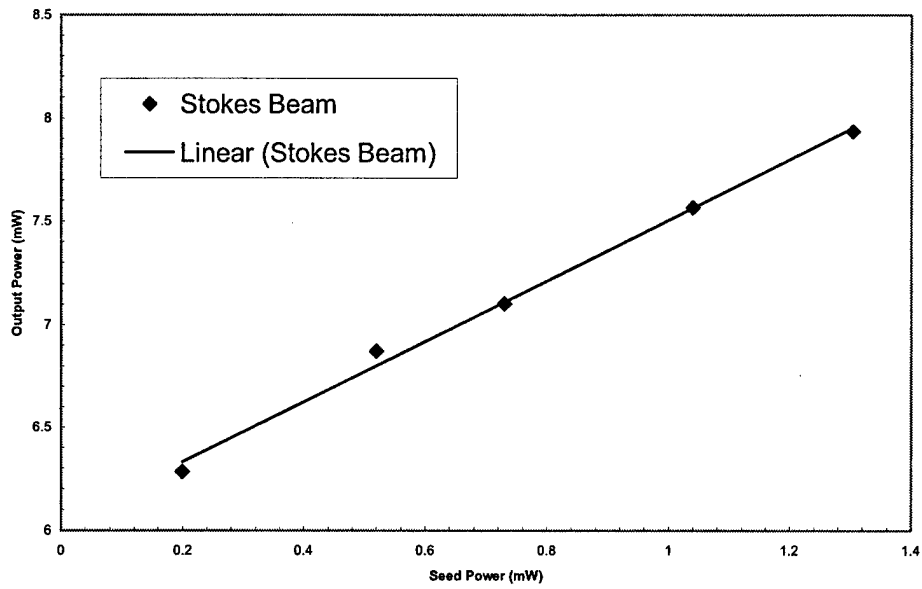


Figure 11. Stokes output versus seed power. Pump power was 32.9 mW

desired power. There are enough data points to see the linear relationship between output power and seed power as shown by the least squares line. Amplifier gain as a function of seed power is shown on a semi-log plot in Figure 12. As expected, the gain for smaller

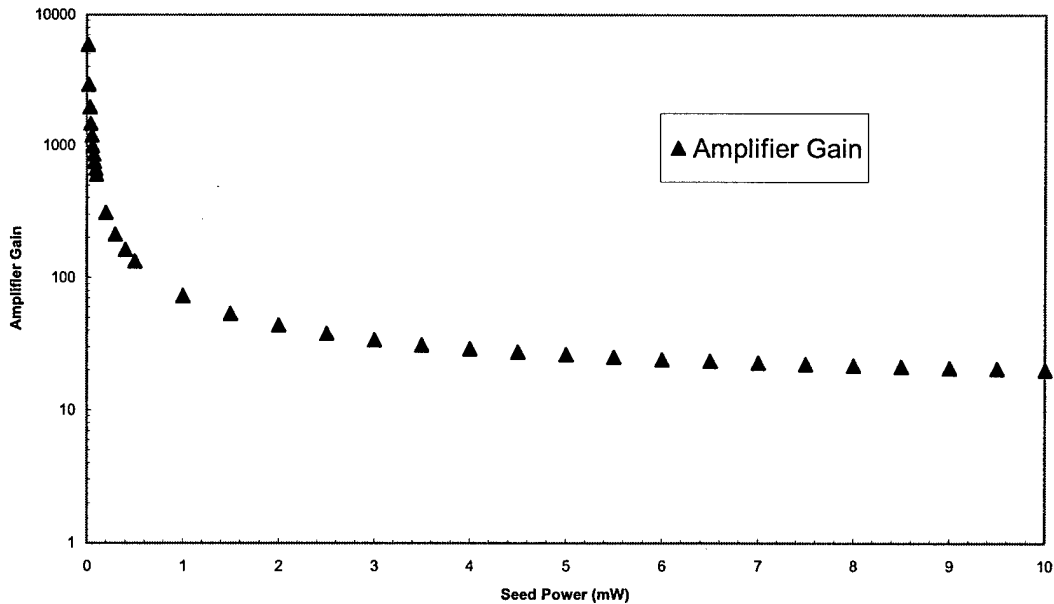


Figure 12. Saturated amplifier gain as a function of seed power. Pump power was 32.9 mW.

seed power increases exponentially.

### 5.3 Brillouin Shift

A spectrum including both pump and Stokes beam is shown in Figure 13. Using Equation 13, the theoretical value of the Brillouin shift is 21.21 GHz. By measuring the shift between the pump and Stokes beam and adding an integer multiple of the free spectral range of the interferometer to achieve a value closest to its theoretical value, the Brillouin shift was estimated to be  $20.92 \pm 0.5$  GHz. As mentioned above, the spectrum of the laser exhibited erratic fluctuations, preventing use of the wavemeter for directly measuring the Stokes wavelength.

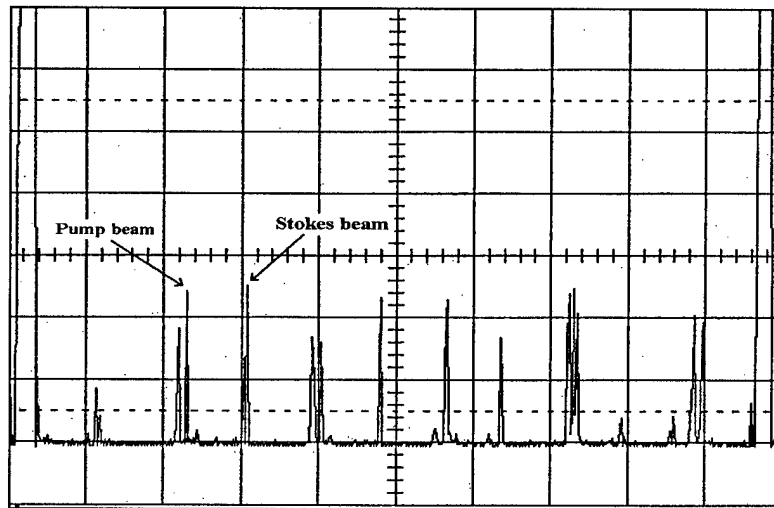


Figure 13. Spectrum of pump and Stokes beams. X-axis is relative frequency and Y-axis is relative intensity.

### 5.4 Beam Profile

Intensity profiles of the output beam are shown in Figure 14. Figure 14a shows

the seed beam that is transmitted through the fiber without pumping. This profile is characteristic of an  $LP_{01}$  mode transmitted through the fiber. Figure 14b shows the amplification of this seed beam. The central portion of the beam was saturated from gain due to SBS. Figure 14c shows the seed beam coupled into an  $LP_{11}$  mode, as evidenced by the dual lobe structure. With pump beam on for the amplifier fiber, the Stokes beam retains the dual lobe structure as shown in Figure 14d.

An acid-etched microscope slide was used to aberrate the pump beam. Figure 15 shows the Fresnel reflections of the unaberrated and aberrated pump beams. The Stokes beam retained the profile of the injected seed beam even with the aberrated pump beam.

Changes in the Stokes beam profile were monitored while adjusting the coupling of the seed beam into the amplifier fiber. Transversely adjusting the end of the fiber relative to the coupling optic changed the beam intensity, but did not alter its shape. Likewise, changing the angle of the seed beam relative to the fiber over a small range did not affect beam quality. It was difficult to adjust the alignment of the seed beam into the amplifier fiber to couple the desired spatial mode, and the occurrence of a particular mode was due more to chance than any other factor.

### *5.5 Polarization of the Stokes Beam*

The polarization of the Stokes beam was also investigated. The seed beam was vertically polarized due to the polarizing beamsplitter used to direct the seed beam to the amplifier fiber, while the pump beam was horizontally polarized. For SBS oscillation, the Stokes beam for a linearly polarized pump beam is polarized the same as the pump beam. In this experiment, however, the polarization of the Stokes beam was the same polarization as the seed beam.

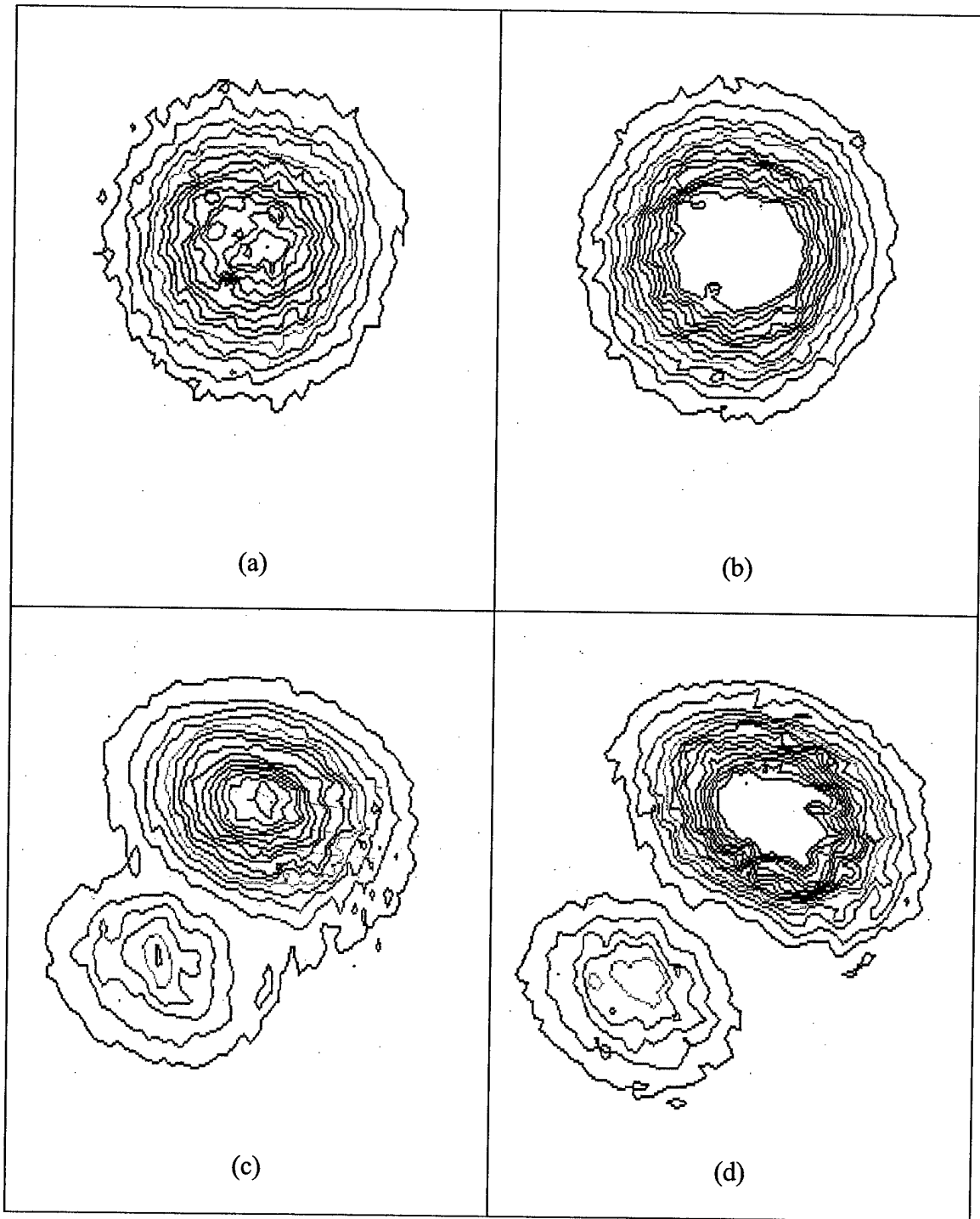


Figure 14. Images of the output beam: (a) LP<sub>01</sub> seed beam without pumping, (b) amplified LP<sub>01</sub> beam, (c) LP<sub>11</sub> seed beam without pumping, and (d) amplified LP<sub>11</sub> beam.

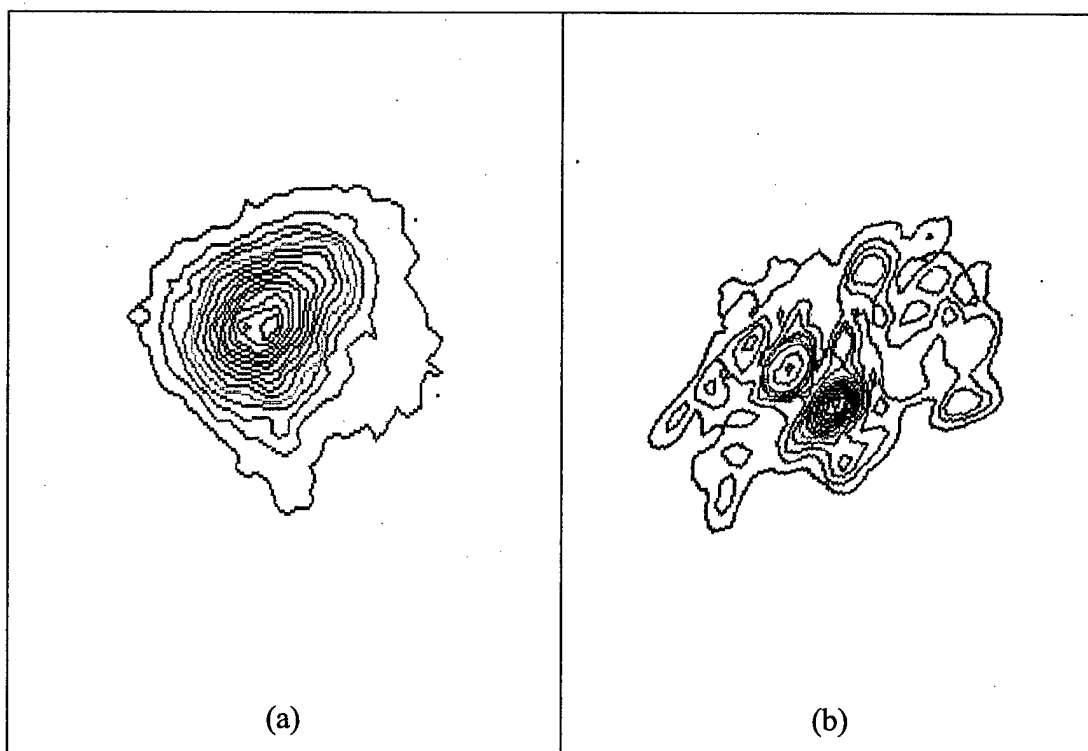


Figure 15. Profile of the Fresnel reflection of the pump beam: (a) unaberrated beam and (b) aberrated beam.

For the vertically polarized seed beam, the Stokes beam was also vertically polarized. Changing the polarization of the seed beam by inserting a half-wave plate affected the shape of the Stokes beam. This is depicted in Figure 16. Figure 16a shows one trial which generated a dual lobe amplified Stokes beam similar to Figure 14d above. Figure 16b shows this same beam after the polarization of the seed beam has been rotated to horizontal. The beam profile changed as the orientation of the half-wave plate was continuously rotated. Further investigation into Stokes beam polarization is warranted to verify the relationship between seed, pump, and Stokes beam polarizations.

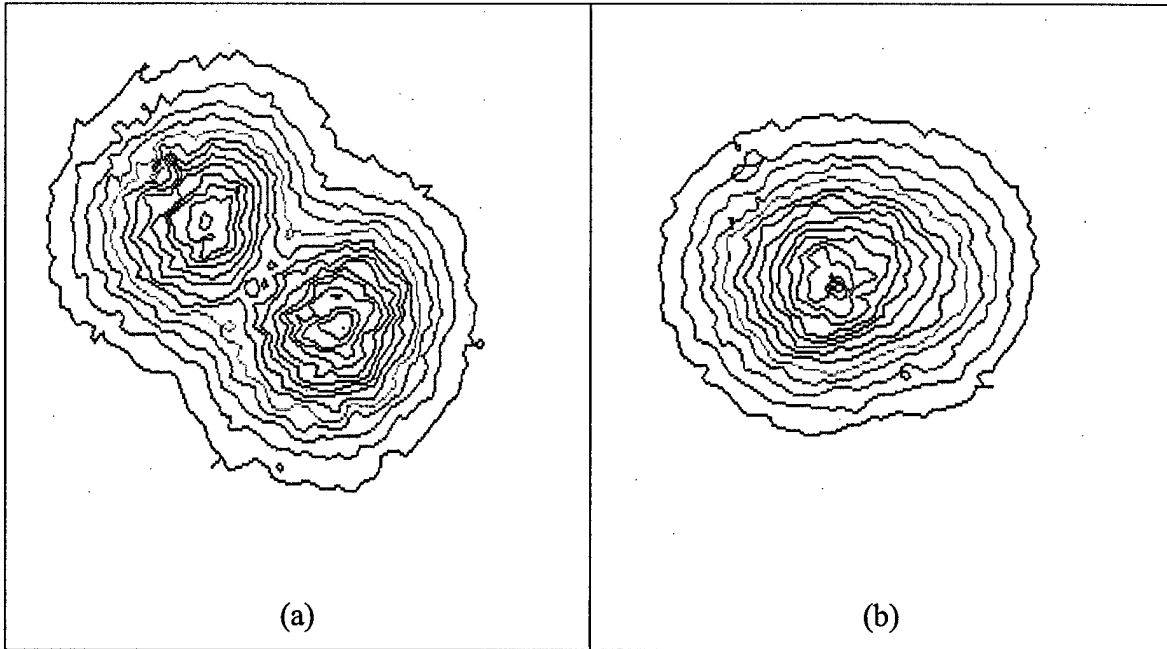


Figure 16. Effects of seed beam polarization on the amplified Stokes beam: (a) amplifier output for an arbitrary rotation of the seed beam polarization and (b) amplifier output when seed beam polarization has been rotated by 90 degrees.

### 5.5 SBS Amplification in 50 $\mu\text{m}$ Fiber

For this experiment, the 9.5  $\mu\text{m}$  fiber used as the amplifier was replaced with the 50  $\mu\text{m}$  fiber. Figure 17 shows the Fresnel reflection, the transmitted seed beam, and the amplifier output with maximum pump power applied. SBS was not observed, nor was there any indication of beam clean-up. Using the same method for determining the Brillouin threshold described in Section 5.1 above, the minimum pump power to support SBS amplification with a 2.23 mW seed beam in the 50  $\mu\text{m}$  fiber would be 148.4 mW. Unfortunately, the laser used in this experiment could not produce enough power to both generate the seed beam in the oscillation fiber and pump the amplifier fiber. However, this minimum pump power is significantly smaller than the estimated 280.7 mW required to initiate SBS oscillation.

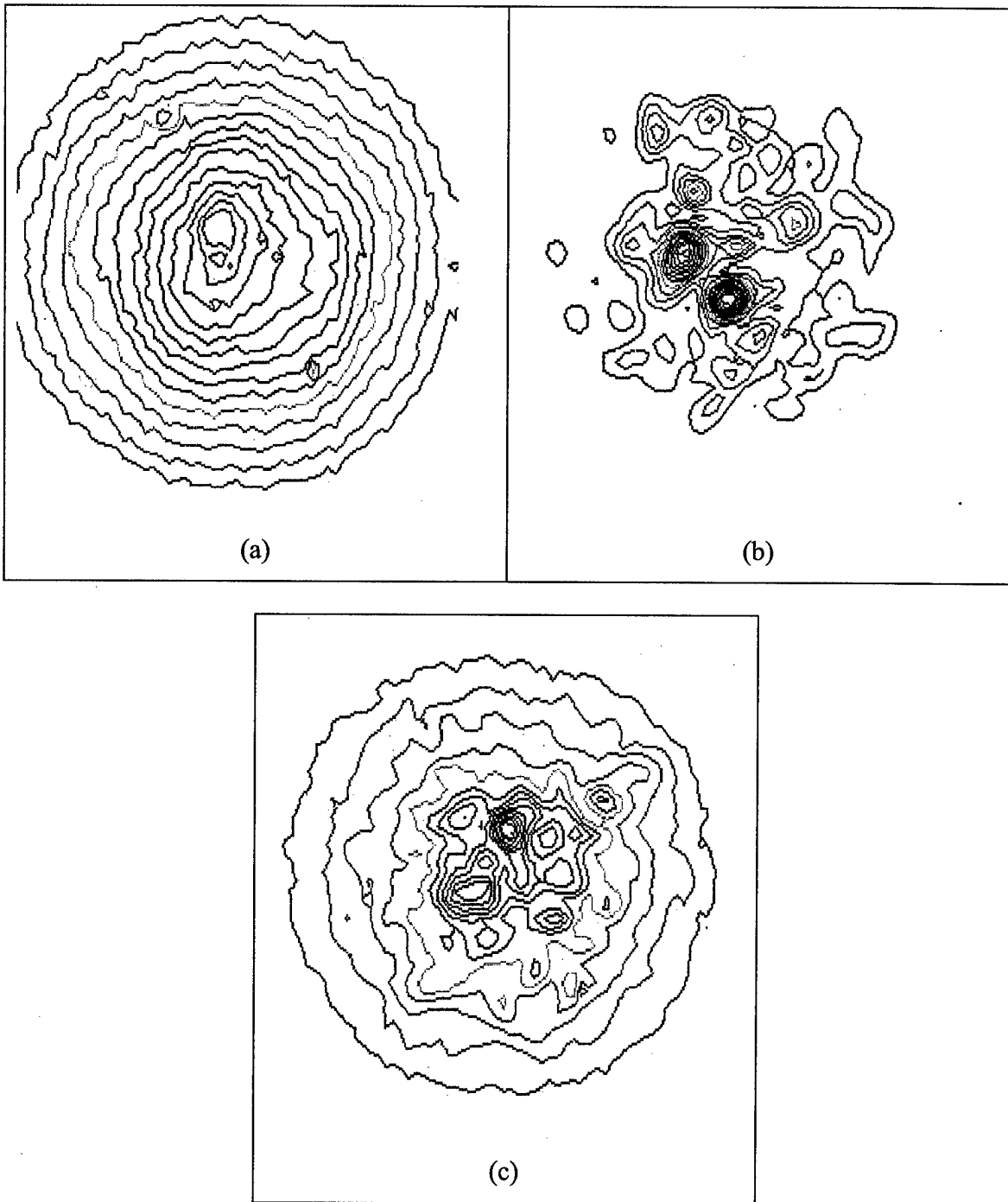


Figure 17. Contour plots of amplifier output for the 50  $\mu\text{m}$  fiber: (a) Fresnel reflection, (b) seed beam only, and (c) amplifier output with maximum pump power applied. SBS does not occur in the 50  $\mu\text{m}$  fiber.

## VI. *Conclusion and Recommendations*

### 6.1 *Conclusion*

By generating a beam at the Stokes frequency in a spool of fiber via SBS oscillation and seeding another spool of the same fiber, SBS amplification was observed in a 9.5  $\mu\text{m}$  core diameter multimode fiber. Brillouin threshold, amplifier gain and spatial coherence of the amplified Stokes beam were measured and compared against previously reported data for SBS oscillation.

Laser beam amplification via SBS does not exhibit the same beam clean-up property as SBS oscillation. The spatial quality of the output beam depended on the polarization and coupling of the seed beam. However, the Stokes beam was unaffected by an aberrated pump beam. While it was possible to generate a beam with a fundamental gaussian profile in the 9.5  $\mu\text{m}$  optical fiber, doing so required precise coupling of the seed beam into the amplifier fiber. Using a larger diameter fiber which supports in excess of a thousand transverse modes would likely increase the difficulty in generating a gaussian beam.

A significant reduction in pump power required to support SBS can be gained by using amplification over oscillation. In the 9.5  $\mu\text{m}$  fiber seeded with a 2.23 mW Stokes-frequency beam, pump power of only 4.10 mW was required to initiate measurable SBS, as opposed to  $\sim 30$  mW reported by Rodgers for SBS oscillation for the same fiber and wavelength. While 4 mW of power is easily achieved by a single diode laser, the minimum pump power to support SBS amplification is estimated to be 148.7 mW for the 4.4 km length of 50  $\mu\text{m}$  fiber used in this experiment. For example, a 100 meter length of

the 50  $\mu\text{m}$  fiber would require 3.232 W of pump power with 5 mW of seed power. In the absence of a seed beam, the same fiber would require in excess of 5 W of pump power to initiate SBS. Conversion efficiency of SBS amplification was 44%, comparable to conversion efficiency reported for SBS oscillation.

The method described by Rodgers to coherently combine multiple beams using SBS oscillation could easily be applied to the case of SBS amplification. By directing multiple pump beams into a seeded fiber, each having power less than the minimum required to support SBS amplification, but whose total power exceeded the minimum, a single Stokes beam would be generated. Without a way of consistently producing a beam with a gaussian profile, however, the use of SBS amplification as a means of beam combining is limited.

## *6.2 Recommendations for Future Research*

One way to take advantage of the lower pump power requirement for the SBS amplification process, but still produce a gaussian beam is to develop a multi-stage beam combining system. If the ultimate goal of combining diode lasers is to produce an output on the order of a kilowatt, it will not be possible to do so using a single fiber. When combining two beams in an optical fiber, the polarization of the beams can be exploited using a polarizing beamsplitter so the two beams enter the fiber co-axially. Ideally, aligning all the pump beams along the same axis provides the most straightforward way of pumping the fiber. However, for more than two beams, this method does not work and some input power will be lost in trying to align the beams co-axially. An alternative method is to direct the beams in the same direction lying adjacent to each other, but not overlapping. This could be accomplished using fiber optic patch cords to collimate the

individual pump beams, or using a diode laser array with a focusing element for each diode laser. The drawback of this method is as more beams are added, the diffraction limited spot size of the pump beam array increases.

SBS amplification would allow the use of large core diameter fibers while requiring significantly less power to coherently combine the pump beams into a single beam. Larger core diameter fibers would allow for maximum coupling of pump beams into a single fiber using the method mentioned above. Using several such amplifiers would generate multiple beams which could then be used to pump a fiber for SBS oscillation. The end result would be a moderate-power, gaussian beam. With conversion efficiencies of approximately 50% for both amplification and oscillation, and assuming coupling efficiencies on the order of 70%, the amplifiers could be cascaded several times and still achieve higher efficiency than a comparable solid-state, gas, or liquid laser system.

By adjusting the seed beam polarization, it was possible to generate a gaussian beam from the SBS amplifier. Since only two modes were observed in the 9.5  $\mu\text{m}$  fiber, it is difficult to generalize the effect of seed beam polarization on beam clean-up via SBS amplification. Further investigation into this effect may provide a more conclusive relationship between seed beam polarization and beam clean-up by SBS amplification.

Different types of fibers should be investigated for their impact on the SBS process. Doped fibers and fibers made of materials other than glass may have different Brillouin gain coefficients and linewidths. Using double clad fibers with a single mode core would ease the coupling constraints for the pump beams and would ensure the amplification process would generate a gaussian beam.

Another extension of this thesis would be to pursue stimulated Raman scattering (SRS) amplification as a means of beam combining. SRS is similar to SBS except the interaction of pump and Stokes waves involves optical rather than acoustical phonons. The Raman gain coefficient is several orders of magnitude smaller than the Brillouin gain coefficient, but the gain bandwidth is on the order of tens of terahertz. Additionally, SRS can occur in the forward direction in optical fibers, which would make it easier to separate the Stokes beam from the pump beam than a backward propagating Stokes beam. In this thesis, the reason for splitting off a portion of the power from the pump laser was to ensure the seed beam would precisely match the Stokes frequency since the Brillouin gain linewidth is on the order of tens of megahertz. In practical applications using different laser sources, such frequency matching would be extremely difficult with SBS, but much more manageable using SRS.

One further recommendation for future research is to utilize a conventional laser source other than a diode laser as a pump. While the motivation behind this work is to combine diode lasers, it would be much easier to use a ~5 W solid-state laser capable of consistently producing a single longitudinal mode to demonstrate beam combining concepts. This would allow for multiple beam combining by splitting off power from the pump laser, with each beam having the same frequency and adequate power to use larger diameter fibers for SBS. Alternatively, a multi-mode laser with sufficient power could be used to pursue SRS amplification.

## Bibliography

1. Agrawal, Govind P. *Fiber-Optic Communication Systems*. New York: John Wiley & Sons, Inc., 1992.
2. Agrawal, Govind P. *Nonlinear Fiber Optics*. San Diego: Academic Press, 1989.
3. Aoki, Yasuhiro and Kazuhito Tajima. "Dependence of the stimulated Brillouin scattering threshold in single-mode fibers on the number of longitudinal modes of a pump laser," *In Tech. Digest, Conference on Lasers and Electro-Optics, CLEO 1987*, Paper TUHH5: 86-87, Baltimore, 1987.
4. Aoki, Yasuhiro, Kazuhito Tajima, and Ikuo Mito. "Observation of stimulated Brillouin scattering in single-mode fibres with single-frequency laser-diode pumping," *Opt. Quantum Electron.*, 19: 141-143 (1987).
5. Bruesselbach, Hans, "Beam cleanup using stimulated Brillouin scattering in multimode fibers," *Conference on Lasers and Electro-Optics, CLEO 1993*, 424-425, 1993.
6. Cotter, D. "Observation of stimulated Brillouin scattering in low-loss silica fibre at 1.3  $\mu\text{m}$ ," *Electron. Lett.*, 18: 495-496 (April 1982).
7. Hecht, Eugene. *Optics* (Third Edition). Reading, MA: Addison-Wesley, 1998.
8. Henry, Wanda M. "Fibre acoustic modes and stimulated Brillouin scattering," *Int. J. Optoelectronics*, 7: 453-478 (1992).
9. Hill, K.O., B.S. Kawasaki, and D.C. Johnson. "cw Brillouin laser," *Appl. Phys. Lett.*, 28: 608-609 (May 1976).
10. Ippen, E.P. and R.H. Stolen. "Stimulated Brillouin scattering in optical fibers," *Appl. Phys. Lett.*, 21: 539-541 (December 1972).
11. Lichtman, E. and A. A. Friesem. "Stimulated Brillouin Scattering Excited by a Multimode Laser in Single-mode Optical Fibers," *Opt. Comm.*, 64: 544-548 (December 1987).
12. Loree, Thomas R. et al. "Phase locking two beams by means of seeded Brillouin scattering," *Opt. Lett.*, 12: 178-180 (March 1987).
13. Rodgers, Blake C. *Laser Beam Combining and Cleanup via Stimulated Brillouin Scattering in Multi-mode Optical Fibers*. MS thesis, AFIT/GAP/ENP/99M-09. School of Engineering, Air Force Institute of Technology (AU), Wright-Patterson AFB, OH, March 1999.

14. Rodgers, Blake C., Timothy H. Russell, and Won B. Roh, "Laser beam combining and cleanup by stimulated Brillouin scattering in a multimode optical fiber," *Opt. Lett.*, 24: 1124-1126 (August 1999).
15. Ryan, Patrick T. *Optical Phase Conjugation via Stimulated Brillouin Scattering in Multimode Optical Fiber*. MS thesis, AFIT/GEP/ENP/90S-1. School of Engineering, Air Force Institute of Technology (AU), Wright-Patterson AFB, OH, September 1990.
16. Saleh, Bahaa E. A. and Malvin Carl Teich. *Fundamentals of Photonics*. New York: John Wiley & Sons, Inc., 1991.
17. Sternklar, Shmuel et al. "Misalignment sensitivity of beam combining by stimulated Brillouin scattering," *Opt. Lett.*, 15: 469-471 (May 1990).
18. Stolen, R. H. "Polarization Effects in Fiber Raman and Brillouin Lasers," *IEEE J. Quantum Electron.*, 15: 1157-1160 (October 1979).
19. Valley, Marcy, Gabriel Lombardi, and Robert Aprahamian. "Beam combination by stimulated Brillouin scattering," *J. Opt. Soc. Am. B*, 3: 1492-1497 (October 1986)
20. Verdeyen, Joseph T. *Laser Electronics* (Third Edition). Englewood Cliffs, NJ: Prentice Hall, 1995.
21. Wong, G. K. N. and M. J. Damzen. "Investigations of Optical Feedback Used to Enhance Stimulated Scattering," *IEEE J. Quantum Electron.*, 26: 139-148 (January 1990).

## *Vita*

Captain Bryan J. Choi was born on 22 August 1972 in San Jose, California. After graduating from high school in 1990, he attended Princeton University in Princeton, New Jersey, earning a Bachelor of Science in Electrical Engineering in June 1994. While at Princeton, he participated in the Air Force Reserve Officers Training Corps program and was commissioned into the Air Force upon graduation. He was assigned as a flight test engineer with the C-135E Argus II aircraft while serving at the Phillips Laboratory, Kirtland Air Force Base, New Mexico (now Air Force Research Laboratory) from September 1994 to August 1998, when he entered the School of Engineering at the Air Force Institute of Technology, Wright-Patterson Air Force Base, Ohio.